Current-Voltage analysis in SDBD plasma discharge

C.Piferi[1], R.Barni[1], H.E.Roman[1] and C.Riccardi[1]

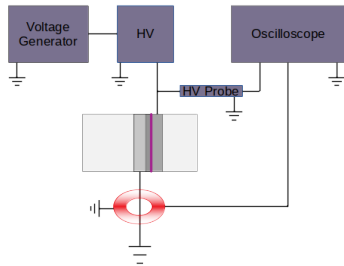[1] *Università degli Studi di Milano-Bicocca, Milano, Italy*

Figure 1: Setup experiment

Our experimental setup consist in a Surface Dielectric Barrier Discharge (SDBD) plasma powered by a radiofrequency (RF) generator coupled with a high voltage (HV) transformer. Our plasma device is composed of a 3 mm thick dielectric barrier in Teflon and pair of 12 cm long conductive electrodes leaning on the two faces of the barrier with 2 cm overlapping. We measure the high voltage with an HV probe and the current with a Rogowski coil placed around the ground HV cable.

We set the voltage of the RF generator in a range of 7-14 V, so that the high voltage converter has an output in 5.6-11.2 kV range. During the data presentation we will refer to the data sets with the corrispondent RF generator voltage value, which are equispaced. The RF generator voltage conversion to HV voltage is in Figure 2. We applied frequencies from a minumum of 32 kHz (if RF voltage is 14 V) to a maximum of 36 kHz (if RF voltage is 7 V).
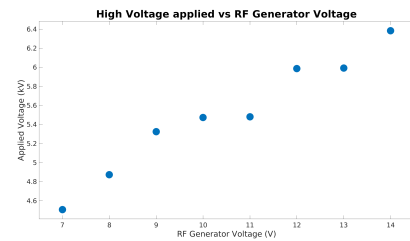

Figure 2: RF vs HV Voltage in our setup experiment.

A Rogowski coil usually consists of a conductor winding wrapped around a toroidal former of non-ferromagnetic material, such as air core. This ensures excellent linearity to the response of the coil due to the absence of saturation.

To use a Rogowski coil as a probe, a cable has to pass through the toroid. The current flowing in the cable generates a voltage variation at the output of the coil proportional to the rate of the change of the current dI/dt. This voltage can be integrated with an integrating circuit, that could be a resistance.

There are some difficulties related to Rogowski coil such as the variation of the coil parameters with temperature and the fact that the coil are not symmetrical so that the measurement depends on the position of the conductor passing through the torus and its orientation.

To avoid this problem, it is possible to use a ferromagnetic coil, and so we did in this work. We used a Rogowski coil with ferromagnetic core (NiZn ferrite N30 with μ_i 4300), with 50Ω integration resistance and 3.5 windings.

We used a 50 cm long RG-59 BNC coaxial cable, calibrated with our Rogowski coil and always used together, and an Agilent Infinium MSO8104A oscilloscope with 1.0 GHz bandwidth and 4 GSamples/s maximum acquisition rate.

The Rogowski coil signal could have two main components: one is the displacement current and the other is due to the plasma. We are only interested in the last one, so we have chosen a probe that suppresses the capacitive component by itself.

After the amplitude calibration, we obtain the attenuation factor to correct our Rogowski response in the bandwidth 10^6-10^8 Hz, i.e.
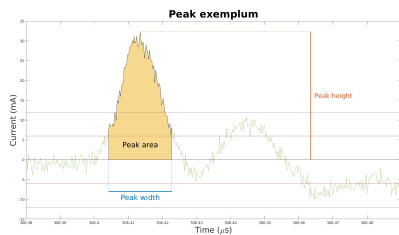
$$\frac{V_{\text{Rogowski}}}{I_{\text{Ref}}} \sim 10 \text{ V/A}$$

where I_{Ref} is the testing current at that frequency.

Phase calibration could be useful to a Fast Fourier Transform analysis to clear the signal, but this kind of analysis requires higher resolution in time.
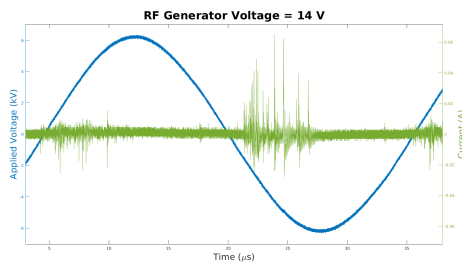
(a)

(b)

Figure 3: (a) Example of temporal acquisition. Left axis (blue line) is applied voltage; right axis is the current measured by Rogowski coil (green line); (b) definition of the parameters.

Every oscilloscope channel acquisition has 4100000 points, sampled every 0.25 ns. Due to the restricted statistics, we needed to save 30 files for each voltage and analyse them all together for a total time span of 30.75 ms. A typical brief temporal acquisition is plotted in Figure 3a; left axis referes to the applied voltage (blue line) and the right axis to the current measured by the Rogowski coil (green line). We performed a fit of the HV signal with a sine function to obtain its properties, such as amplitude, frequency and argument at each point. Due to the setup, the current always has the same sign of the electric field.

From the current signal we deduce properties of the spikes, such as maximum intensity, time duration and HV phase position. It is also important to discern if a peak is real or just an artifice due to the probe. To cut out the background, we choose 2σ threshold, where σ is the standard deviation of all the Rogowski coil data. We mark a peak as signal if it passes 4σ threshold; its time duration, also named as **peak width**, is evaluated at 2σ threshold, its maximum intensity (**peak height**) from the zero level, the **HV phase position** is the relative position of the

maximum and the current carried by the peak (**peak area**) is the sum of the intensity of each acquisition occurred in the peak's time duration, as shown in Figure 3b.

These are filamentary discharges with several microdischarges which have a duration of the order of ten nanoseconds and the height of about ten milliampers.

We count all the peaks and we histogram them depending on the HV phase position. We can notice four different phase regions, two with the presence of the current spikes and two without them. The **forward stroke** is between 0 and π and the **backward stroke** is from π to 2π. The number of events in the forward stroke is much lower than in the backward stroke,

Figure 4: Peaks counts vs HV phase.

where we see that when the RF voltage grows the peak distribution focuses on the breakdown area.
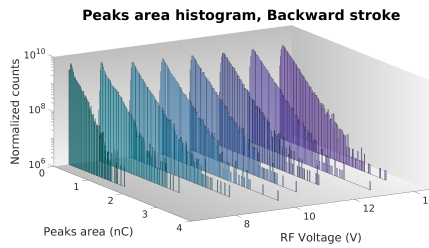
(a)
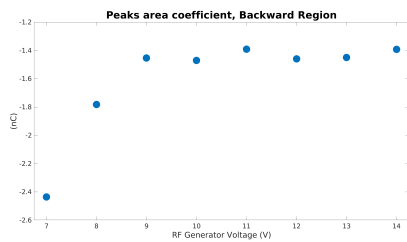
(b)

Figure 5: (a) Distribution of peak area; (b) exponential coefficient of the decrease.

The statistics of the forward stroke is not sufficient and for this reason we will only investigate the distribution of data referring to the backward stroke.

The area distribution (Figure 5a in semilog-z representation), which is the distribution of the charge carried by each peak, has an exponential decrease RF voltage dependent (Figure 5b). The typical dimension of the peak area is 0.3 nC for the backward stroke and -0.1 nC for the forward one.

The mean peak height is about 35 mA in backward stroke and -20 mA in forward stroke. The height distributions show a similar trend to the area ones.

On the other hand, the peak width, which is the life span of the peak, has a really different distribution: it is strictly non-Gaussian with a lot of events at a long time duration,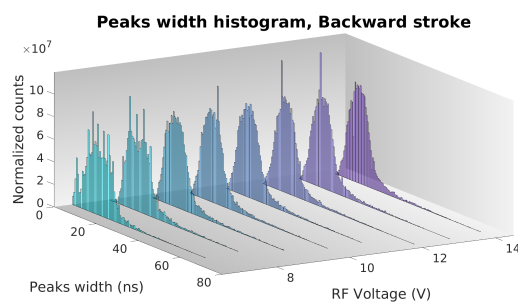 as the kurtosis indicates (Figure 6 and Table 1 for backward stroke). The mean duration of the peak in backward stroke slowly increases with the RF Voltage applied and is about 15 ns; in the forward stroke, the peak width is about 11 ns regardless of the voltage.

It is also interesting to estimate the mean current and the energy carried at each HV voltage cycle. As shown in Figure 7, both charge and energy carried by the plasma are really different

Peaks width histogram, Backward stroke

RF Voltage (V)	Mean (ns)	Kurtosis
7	12.736	5.9485
8	15.123	9.0059
9	15.799	12.2581
10	15.895	11.7833
11	15.953	11.6681
12	16.108	12.9333
13	16.195	11.8495
14	16.293	12.4906

Figure 6: Distribution of peak width.

Table 1: Mean and kurtosis of backward peak height distribution.

in forward and backward stroke. The typical scale of backward stroke charge and energy per cycle is 15 times bigger than the forward ones, for this and a legibility reason the plotted quantities for the forward stroke are scaled of a factor 15. Charge and energy per cycle in forward stroke are quite constant with the RF voltage applied, while there is a linear relation in the backward stroke. Backward stroke charge has a cut-off at 3.73 V and energy at 4.59 V, consistently implemented in the fitting curves (where $Q_{\text{per cycle}}$ is in nC and $E_{\text{per cycle}}$ in μJ)

$$Q_{\text{per cycle}} = 0.8968V - 3.3455 \qquad E_{\text{per cycle}} = 5.1525V - 23.6590$$
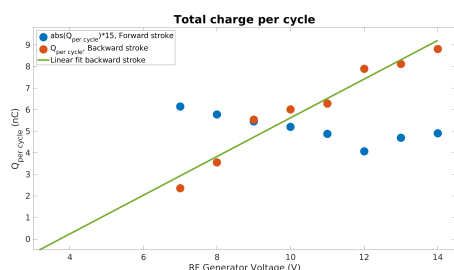
(a)
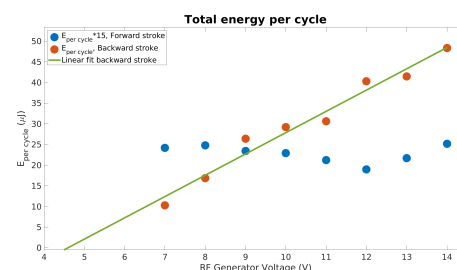
(b)

Figure 7: (a) Mean charge and (b) mean energy per HV cycle.

The aim of this propedeutical work was to investigate the best electrical conditions for our further experiments. This system indeed was developed to break chemical bonds in volatile organic compounds (VOC) in order to reduce air pollution.

References

[1] I.Biganzoli, R.Barni, and C.Riccardi, Review of Scientific Instruments, **84**, 1 (2013), 10.1063/1.4773233

[2] I.Biganzoli, Ph.D. Thesis, Characterization of Atmospheric Pressure Plasmas for Aerodynamic Applications

[3] I.Biganzoli, R.Barni, C.Riccardi, A.Gurioli, and R.Pertile, Plasma Sources Sci. Technol. **22** 025009 (2013)

[4] I.Biganzoli, R.Barni, and C.Riccardi, J. Phys. D: Appl. Phys. **46** 025201 (2013)

[5] R.A.Siliprandi, H.E.Roman, R.Barni, and C.Riccardi, J. Appl. Phys. **104**, 063309 (2008), 10.1063/1.2978184